

Light-dependent conformational change of neoxanthin in a siphonous green alga, *Codium intricatum*, revealed by Raman spectroscopy

Chiasa Uragami · Denise Galzerano · Andrew Gall · Yusuke Shigematsu ·
Maiwen Meisterhans · Naohiro Oka · Masahiko Iha · Ritsuko Fujii ·
Bruno Robert · Hideki Hashimoto

Received: 13 December 2013 / Accepted: 2 May 2014 / Published online: 27 May 2014
© Springer Science+Business Media Dordrecht 2014

Abstract Siphonous green algae, a type of deep-sea green algae, appear olive drab and utilize blue–green light for photosynthesis. A siphonous green alga, *Codium (C.) intricatum*, was isolated from Okinawa prefecture in Japan, and a clonal algal culture in filamentous form was established. The major light-harvesting antenna was analogous to the trimeric LHCII found in higher plants, but the *C. intricatum* complex contained an unusual carbonyl carotenoid siphonaxanthin. Culture conditions were optimized to achieve high siphonaxanthin content in intact lyophilized filamentous bodies. Interestingly, the carotenoid composition was different when cultured under high irradiance: all-*trans* neoxanthin was accumulated in addition to the normal 9'-*cis* form in whole cell extract. Resonance Raman spectra of intact filamentous bodies, cultured under high- and low-light conditions, confirmed the accumulation of all-*trans* neoxanthin under high irradiance conditions. A plausible function of the presence of all-*trans* neoxanthin will be discussed in relation to the regulation against high light stress.

Keywords Photosynthetic antenna · Xanthophyll · Green algae · Siphonaxanthin · Raman spectroscopy

Abbreviations

C	Codium
Sx	Siphonaxanthin
Sn	Siphonaxanthin ester
tNx	All- <i>trans</i> neoxanthin
9cNx	9'- <i>cis</i> neoxanthin
Vx	Violaxanthin
Chl	Chlorophyll

Introduction

Several species of green algae, designated siphonous green algae, are a deep drab color and utilize green light for photosynthesis (Anderson 1983). This coloration and

C. Uragami · Y. Shigematsu · R. Fujii · H. Hashimoto (✉)
Graduate School of Science, Osaka City University, 3-3-138
Sugimoto, Sumiyoshi-ku, Osaka 558-8585, Japan
e-mail: hassy@ocarina.osaka-cu.ac.jp

R. Fujii
e-mail: ritsuko@ocarina.osaka-cu.ac.jp

C. Uragami
Japan Society for the Promotion of Science, 4-1-8 Honcho,
Kawaguchi, Saitama 332-0012, Japan

D. Galzerano · A. Gall · M. Meisterhans · B. Robert
Institute of Biology and Technology of Saclay, CEA
(Commissariat à l'Énergie Atomique), URA 2096 CNRS (Centre
National de la Recherche Scientifique), 91191 Gif sur Yvette,
France
e-mail: bruno.robert@cea.fr

N. Oka · M. Iha
South Product Co. Ltd., 12-75 Suzaki, Uruma,
Okinawa 904-2234, Japan

R. Fujii · H. Hashimoto
The Osaka City University Advanced Research Institute for
Natural Science and Technology (OCARINA), 3-3-138
Sugimoto, Sumiyoshi-ku, Osaka 558-8585, Japan

R. Fujii
Japan Science and Technology Agency, Precursory Research for
Embryonic Science and Technology (JST-PRESTO), 4-1-8
Honcho, Kawaguchi, Saitama 332-0012, Japan

wavelength utilization are caused because the carotenoid siphonaxanthin (Sx) and its ester (Sn) take the place of lutein in LHCII-type photosynthetic antenna complexes (Wang et al. 2013). These siphonous green algae inhabit the subtidal zone of seashores, where irradiance conditions fluctuate drastically because of changes in water column depths. The adaptations of siphonous green algae to these fluctuations in irradiance conditions have not been studied closely because these algae normally grow into large and spongy bodies; consequently, they are difficult to culture. Recently, we developed a culture method for propagation of a filamentous form of *Codium* (*C.*) *intricatum* OKAMURA, a siphonous green alga (Oka et al. 2012). This culture method is optimized to obtain higher Sx/Sn yields in lyophilized cells. During the optimization process, we found that the pigment composition is affected only when extremely high light intensities were used during culture.

Sx-chlorophyll *alb* protein (SCP) constitutes the light-harvesting complexes of siphonous green algae. SCPs have been isolated, and the pigment composition has been investigated. The chemical structures of all the carotenoids of *C. intricatum* are pictured in Fig. 1. The characteristic carbonyl carotenoid, Sx, Sn, or both are the major light-harvesting carotenoids; moreover, α -carotene takes the place of β -carotene (Anderson 1983; Chu and Anderson 1985). Xanthophyll cycle carotenoids violaxanthin (Vx)

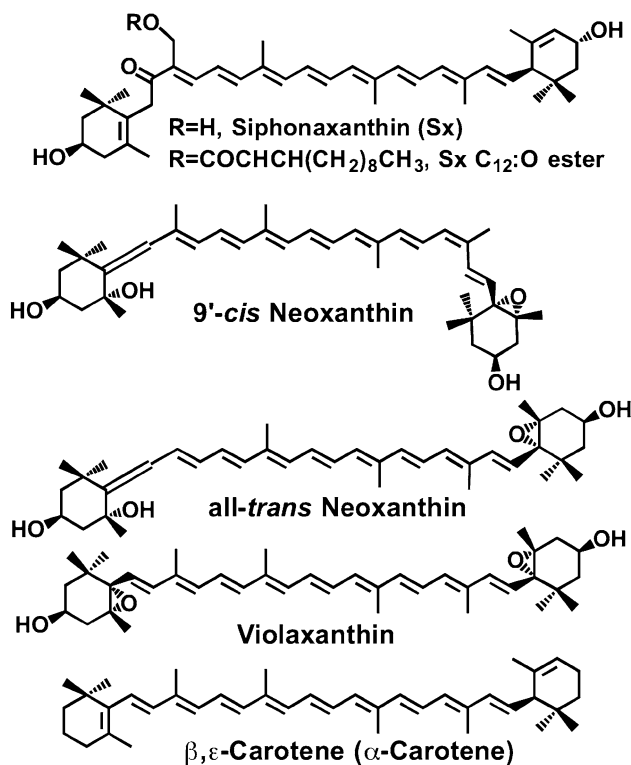


Fig. 1 Chemical structures of the carotenoids in *C. intricatum*

and neoxanthin (Nx) are also present (Yokohama 1983). The Nx in natural oxygenic photosynthetic organisms takes the 9'-*cis* Nx (9cNx) conformation (Takaichi and Mimuro 1998). Notably, an additional pigment is evident when intact cultivated filamentous *C. intricatum* cells are grown under extremely high light intensities, and this pigment is probably all-*trans* Nx (tNx) based on its elution time and absorption spectrum.

Resonance Raman spectroscopy is a powerful method for distinguishing between *cis* and *trans* conformations of carotenoids in solution (Koyama and Fujii 1999) and in pigment-protein complexes (Robert 2009; Andreeva et al. 2004). In the LHCII of plants, one 9cNx and two all-*trans* lutein are bound with an unstoichiometric number of all-*trans* Vx (tVx), and the key Raman signals of 9cNx can be clearly identified (Ruban et al. 2000, 2001; Snyder et al. 2004). Excitation wavelength dependences of the resonance Raman signals have been used to assign the absorptive transitions of each xanthophyll in LHCII complexes. Moreover, Raman signals of lutein have been empirically assigned in relation to the oligomeric/trimeric/monomeric LHCII in plants (Ruban et al. 2000, 2007).

In this study, we used resonance Raman spectroscopy to examine intact filamentous *C. intricatum* cells cultivated under high- and low-light intensities to determine the conformations of the carotenoids in these cells.

Experimental

Culture of filamentous *C. intricatum*

C. intricatum OKAMURA was collected at Okinawa prefecture, Japan, and the clonal algal cultures were established via the micropipette-washing method (Aruga et al. 2000). For one week, filamentous bodies were pre-cultured at 30 °C under a 12–12 h light cycle with 60 $\mu\text{mol m}^{-2} \text{s}^{-1}$ photosynthetic photon flux density (PPFD) in filtered, sterilized sea water with 0.05 % (v/v) TSP₂₉ medium (South Product, Inc., Okinawa, Japan) and continuous bubbling aeration. The only difference between the culture conditions for the two types of cultures (high versus low light intensity) was the irradiances: high (500 PPFD) versus low (20 PPFD) irradiance. Cells were harvested by centrifugation (Kubota 7780) and frozen at –20 °C until analysis.

Pigment extraction

Frozen filamentous cells were lyophilized in a FDU-2100 freeze dryer with a dry chamber (TOKYO RIKAKIKAI CO, LTD, Tokyo, Japan) before pigment extraction. Lyophilized whole cells were homogenized in dimethyl formamide (DMF, Merck) on ice, and homogenates then

were subject to centrifugation. The supernatant (whole extracts) was immediately injected for HPLC analysis.

High-performance liquid chromatography (HPLC)

A reversed-phase HPLC column (Inertsil ODS-P (5 μm), 4.6 \times 150 mm, GL Science Inc.) was equilibrated with eluent A (methanol, acetonitrile, and water at a 9:7:4 (v/v/v) proportional relationship). Samples (20 μl) were injected to the HPLC equipped with a photo-diode array detector (SPD-M20A, Shimadzu, Kyoto, Japan). A linear gradient of eluent B (acetonitrile and ethyl acetate at a 3:7 (v/v) ratio) was then run through the column with flow rate of 0.8 ml/min from 5 to 25 min after injection. Absorption data for a 300–800 nm region were recorded during the HPLC run via both the D₂ and W lamps. LC–APCI–MS spectrometry was performed with a quadrupole MS spectrometer (JMS-700T, JEOL, Japan) equipped with an atmospheric-pressure chemical ionization (APCI) ion source (4.0 kV, 400 °C at needle) and the HPLC system. Peaks were assigned chemical identities based on the results of the LC–APCI–MS spectrometry, HPLC elution pattern, and absorption spectra (see Fig. 2). For each culture, three independent extractions followed by HPLC analyses were used to calculate pigment composition.

Absorption spectra at 77 K

Frozen filamentous cells were suspended in 60 % glycerol–buffer, and absorption spectra at 77 K were recorded with a

Varian Cary E5 spectrophotometer. The spectra were normalized relative to the glycerol–buffer standard; following removal of the glycerol–buffer baseline. The resulting spectra were plotted. The second derivatives of the absorption spectra with respect to wavenumber was computed using the Igor Pro 6.33 J program package followed by spectral smoothing (see Fig. 3b).

Resonance Raman spectroscopy

Frozen filamentous cells were placed on the sample plate and inserted into a liquid nitrogen flow cryostat (Air Liquide). Excitation lights (457.9, 476.5, 488.0, 496.5, 501.7, 514.5, and 528.7 nm) were generated with a 24 W Ar⁺ Sabre laser (Coherent, Palo Alto, CA); the 441.6 nm excitation light was generated with a Liconix He–Cd laser. The 90° scattering from each sample was focused onto a Raman spectrometer (U1000, Jobin–Yvon, France) equipped with a blue-sensitive back-illuminated liquid nitrogen-cooled CCD camera (Spectrum One, Jobin–Yvon, France).

Results and discussion

Pigments in intact filamentous *C. intricatum* cells

The natural irradiance conditions for *Codium* species fluctuate drastically because they inhabit the subtidal zone. We successfully cultivated a filamentous form of one *Codium* species, *C. intricatum* OKAMURA, to study pigment

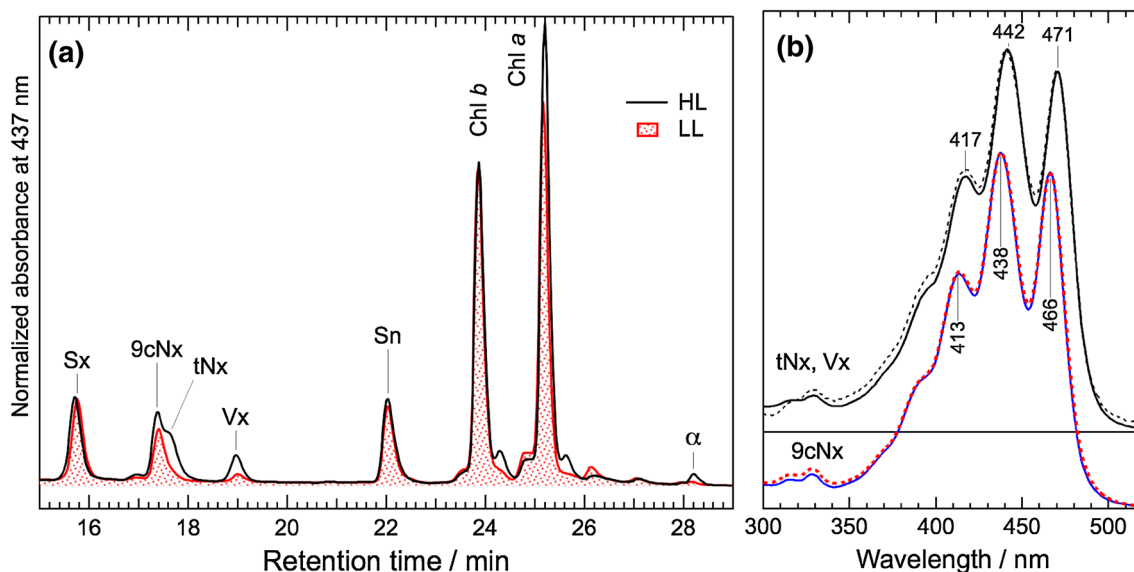


Fig. 2 **a** HPLC profiles of all pigments from intact filamentous *C. intricatum* cells cultivated under HL (black solid line) or LL (red solid line with hash). Profiles were normalized relative to the Sn peak at 22 min. **b** Absorption spectra of 9cNx (dashed line for HL cell and

solid line for LL cell), tNx (solid line) and Vx (dashed line) in HPLC eluent. (See text) (Sx siphonaxanthin, 9cNx 9'-cis neoxanthin, tNx all-trans neoxanthin, Vx violaxanthin, Sn siphonaxanthin ester, α , α -carotene)

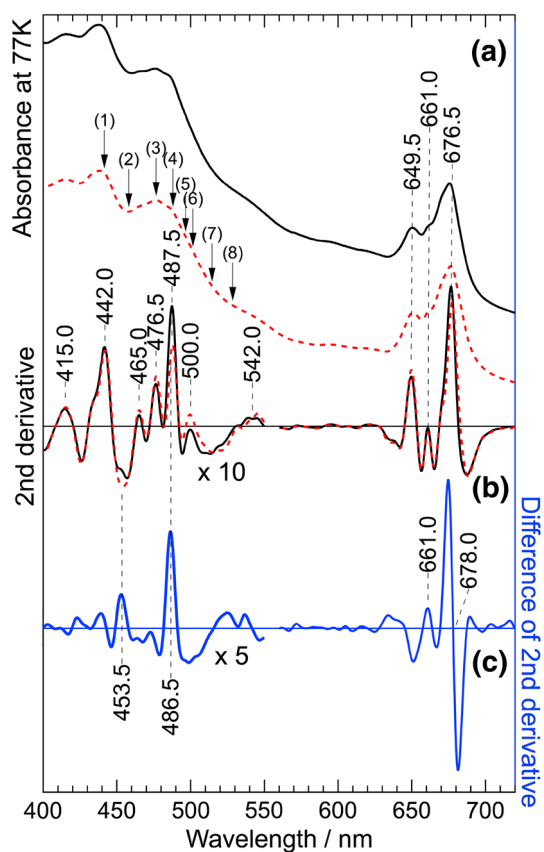


Fig. 3 **a** 77 K Absorption spectra of samples from intact filamentous *C. intricatum* cells cultivated under HL or LL (black solid and dashed red lines, respectively), **b** their second derivatives ($\times -100$), and **c** difference spectrum ($\times -300$) of the second derivatives (HL minus LL) (See Experimental section for further information). Carotenoid regions of (**b**) and (**c**) are magnified relative to the chlorophyll region by the factors indicated. Excitation wavelengths for the Raman spectra are indicated by numbered arrows (See Fig. 5)

composition under multiple controlled light conditions. The filamentous form is rich in chloroplasts and lacks the tough outer structure that protects against dehydration; therefore, it is ideal for the direct detection of intact thylakoid membranes.

HPLC elution profiles of whole pigments from cultivated *C. intricatum* grown under high-light (HL) and low-light (LL) conditions are shown (Fig. 2a). Each HPLC peak associated with samples extracted from LL cells was assigned a definite pigment identity based on retention time and absorption spectrum; these samples contained Sx, 9cNx, Vx, Sn, Chl *b*, Chl *a*, and α -carotene (α). With the HL samples, an additional peak was evident just after the 9cNx peak; this peak had absorption maxima at 472, 443, and 415 nm in HPLC eluent (Fig. 2b). This peak with three absorption maxima was assigned to tNx based on previous studies (Takaichi and Mimuro 1998; Snyder et al. 2004). LC-APCI-MS signals for tNx and 9cNx contained

identical bands (MH^+ , 601 m/z; $MH^+ - H_2O$, 583 m/z; and $MH^+ - 2H_2O$, 565 m/z), confirming this assignment. The tNx peak increased when extracts from intact cells were incubated in light for a few hours (data not shown). This means isomerization from 9cNx to tNx may occur under ambient condition. Therefore the reproducibility was precisely investigated under strict extraction conditions, i.e., dim light, ice temperature, and quick extraction, to draw this result. Thus, we concluded that tNx and 9cNx accumulated during cultivation under HL condition, but only 9cNx accumulated under LL conditions.

The carotenoid composition of each culture type was calculated using values reported for the molar extinction coefficients and absorption spectra in HPLC eluent (Table 1). Note that in the binary HPLC system the HPLC eluent means a mixture of eluent A and B at the retention time. All values are in relative and in arbitrary units; the value for Sn was set to 1. For HL cells, both 9cNx and tNx were calculated as 9cNx. The mixing of the HPLC peaks representing 9cNx and tNx were simulated; the peak shape of 9cNx in the HPLC profile of LL cells was used as that of both 9cNx and tNx, and magnitude and retention time were adjusted to fit real HPLC peaks of HL cells. As a result, the relative area of 9cNx/tNx in the HL profile was found to be 2.2/1.0. The composition of 9cNx (tNx) in HL cell was calculated accordingly to be 0.8 ± 0.1 (0.4 ± 0.1). Therefore, the amount of tNx in LL was clearly lower than that in HL cells, but the amount of 9cNx was the same in the two cell types. Additionally, accumulations of Vx and α -carotene were also higher in HL cells than in LL cells.

Low-temperature absorption spectra

The absorption spectra of intact filamentous cells were recorded at 77 K (Fig. 3). The absorption spectra of intact cells (or chloroplasts) represent the characteristics of the major constituent, the SCP (Anderson 1983). Absorption spectra of HL (upper solid black line) and LL (lower dotted red line) cells were very similar, but the scattering backgrounds differed. The second derivatives were useful for identifying peak positions. Figure 3b shows the second derivatives of the absorption spectra. Importantly, the sign of data was flipped, hence the peak of the second derivative indicates the peak of original absorption spectrum. The spectrum representing the difference of the second derivatives is also shown to emphasize the meaningful differences in the original spectra (Fig. 3c).

In the near-infrared region, second derivative peaks were observed at 676.5, 661.0, and 649.5 nm (Fig. 3b). The 676.5 nm peak can be assignable to the characteristic peak of photosystems reported at 675.0 nm in intact chloroplast (Anderson 1983). The shoulder around 670.0 and 661.0 nm peak can be assignable to the characteristic

Table 1 Carotenoid compositions of intact filamentous *C. intricatum* cells cultivated under HL or LL conditions

	Sx	Nx	Vx	Sn	α -Car
HL	0.98 \pm 0.04	1.18 \pm 0.04	0.30 \pm 0.02	1.00 \pm 0.06	0.07 \pm 0.04
LL	1.04 \pm 0.05	0.72 \pm 0.02	0.10 \pm 0.004	1.00 \pm 0.05	0.02 \pm 0.01
$\epsilon/10^3$	136.9 ^a	135.7 ^b	132.8 ^c	130.9 ^d	123.2 ^e

Three independent injections were averaged and normalized at Sn as 1.00 (see text)

^{a–e} Molar extinction coefficients (ϵ) of the eluent at 437 nm were calculated by using absorption spectra in the HPLC eluent from the reported extinction coefficient (Jeffrey et al. 1997, 2005)

^a Sx 150 at 445 nm in acetone

^b Nx 136 at 438 nm in ethanol

^c Vx 144 at 442 nm in acetone

^d Sn 150 at 462 nm in ethanol

^e α -Car 145 at 448 nm in acetone

peaks of the SCP reported at 669 and 660 nm for isolated SCP (Anderson 1983). The spectrum representing the difference of the second derivatives shows two significant features: one feature is a first-derivative type sigmoid shape at 678.0 nm, and the other is positive enhancement at 661.0 nm. The sigmoid shape can be explained as a blue shift at 678.0 nm peak in the original absorption spectra. The positive enhancement can be explained as an increase in intensity at 661.0 nm peak in the original absorption spectra. Near-infrared absorption peaks were sensitive to the assembly of Chl *a* pigment in the pigment–protein complexes. Thus, both an increase in the magnitude of the 661.0 nm peak and the blue shift at the 678.0 nm peak with HL samples versus LL samples can be explained as an increase in the number of SCPs relative to the number of photosystems under HL conditions.

In the visible-light region, a peak characteristic of SCPs was clearly observed at 542.0 nm in the second derivative spectra (Fig. 3b). This peak could be definitely assigned to Sn/Sx binding (Yokohama 1983). The 487.5, 476.5, and 465.0 nm bands in the second derivative spectra could be assigned to a mixture of the component carotenoids, 9cNx, Sn/Sx, Vx, and α -carotene. The carotenoid peaks from plant LHCII have been clearly documented by Ruban et al. 2000, and the complete absence of a 495 nm peak from our spectrum was consistent with their conclusion that the 495 nm peak represents lutein. In the spectra representing the difference of the second derivatives (Fig. 3c), two clear peaks were evident at 486.5 and 453.5 nm. These peaks indicated notable increases in intensity at both wavelengths in HL cells, and they had an interval of 1,544 cm^{-1} , suggesting 0–0 and 0–1 vibrational transitions of a single carotenoid. Consequently, both peaks can be originated to a single carotenoid that increases in HL cells. The absorption spectra of tNx and Vx were almost identical (Fig. 2b); therefore, the increasing carotenoids represented by the 486.5 and 453.5 nm bands were assigned to both tNx and

Vx (See Table 3). Notably, the absorptive transitions were determined based on the π electron-conjugated systems; consequently, we could not distinguish between tNx and tVx with this spectroscopy.

Resonance Raman spectra

Resonance Raman spectra of filamentous whole cells of *C. intricatum* grown under HL and LL conditions excited at 496.5 nm are shown in Fig. 4. Both spectra showed Raman lines characteristic of carotenoids: C=C stretching (str.) mode (ν_1) appears around 1,500 cm^{-1} , C–C str. mode (ν_2) appears around 1,100–1,240 cm^{-1} , methyl rocking mode (ν_3) appears around 1,000–1,010 cm^{-1} , and C–H out-of-plane wagging mode (ν_4) appears around 950–970 cm^{-1} (Robert 2009). These bands are sensitive to both conformation and structure of carotenoids; therefore, the

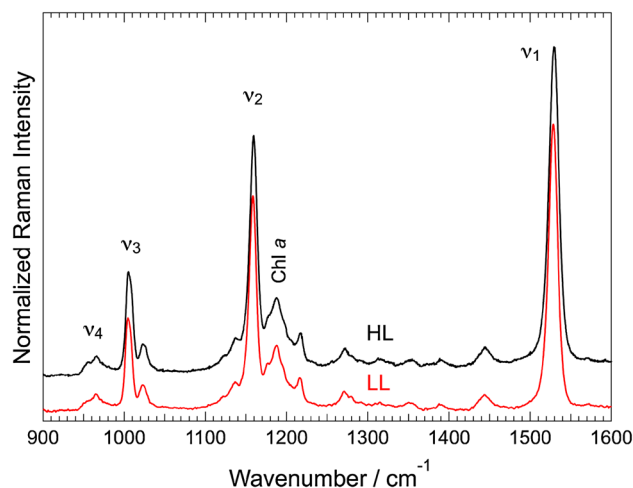


Fig. 4 77 K Resonance Raman spectra of samples from intact filamentous *C. intricatum* cells cultivated under HL or LL (black and red solid lines, respectively) both excited at 496.5 nm

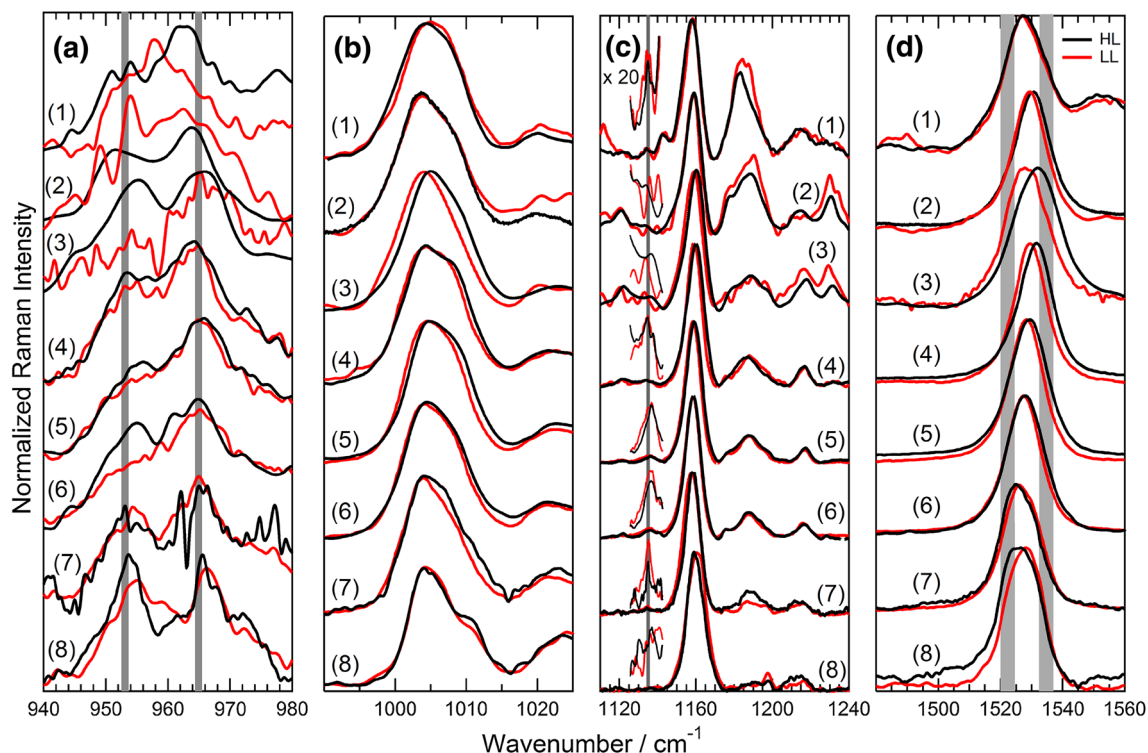


Fig. 5 77 K Resonance Raman spectra of samples from intact filamentous *C. intricatum* cells cultivated under HL or LL (black and red solid lines, respectively). The **a** v_4 , **b** v_3 , **c** v_2 and **d** v_1 regions

of the spectra are shown separately. Excitation wavelengths were (1) 441.6, (2) 457.9, (3) 476.5, (4) 488.0, (5) 496.5, (6) 501.7, (7) 514.5, and (8) 528.7 nm for each region

excitation wavelength dependences of the Raman spectra are useful for assigning absorptive transitions of carotenoids bound to pigment–protein complexes.

The $v_1 \sim v_4$ region of the Raman spectra of HL samples were compared with those of LL samples (Fig. 5); all samples were excited with eight different laser-generated wavelengths (441.6, 457.9, 476.5, 488.0, 496.5, 501.7, 514.5 and 528.7 nm, see arrows in Fig. 3a). Figure 5d shows the v_1 Raman lines which are sensitive to both conjugation lengths (Mendes-Pinto et al. 2013) and to *cis-trans* configurations (Koyama and Fujii 1999; Robert 2009). The v_1 Raman lines of xanthophylls bound to higher plant-type LHCII have been precisely assigned, and 9cNx results in lines at 1,532–1,535 cm^{-1} that change slightly in energy depending on excitation wavelengths (Ruban et al. 2001). The v_1 Raman lines of xanthophylls in the LHCII are close enough to result in one peak when present together; therefore, the plot of the peak frequencies against excitation wavelength can be helpful for evaluating the contribution of each xanthophyll.

In *C. intricatum*, Sx and Sn substitute for lutein, and α -carotene substitutes for β -carotene. Based on the structural similarities and the similarities of the absorption spectra in solution, the v_1 Raman frequency of both Sx and Sn can be quite similar to that of fucoxanthin, i.e., approximately 1,533 cm^{-1} in solution and approximately 1,529 cm^{-1} in

the pigment–protein complexes, FCP (fucoxanthin–chlorophyll *a/c* protein) (Premvardhan et al. 2009). Also, α -carotene may have a v_1 Raman frequency very similar to that of lutein; the v_1 Raman frequency is 1,522–1,524 cm^{-1} (Ruban et al. 2001).

The v_1 peak maxima at the eight different excitation wavelengths were plotted for HL and LL samples (Fig. 6a). With LL samples, the resonance Raman profile was similar to that of higher-plant type trimeric LHCII (Ruban et al. 2000); the higher frequency was around 1,529–1,530 cm^{-1} at both 457.9 and 488.0 nm excitations, and the lower frequency was around 1,527–1,528 cm^{-1} at 441.6/476.5/501.7 nm excitations. These higher and lower frequencies may have occurred because the contribution of 9cNx to the v_1 Raman line was enhanced with excitation wavelengths of 457.9 and 488.0 nm and the contributions of Sx/Sn to v_1 were enhanced with excitation wavelengths of (441.6)/476.5/501.7 nm. In HL cells, the excitation-wavelength dependences were rather unclear between excitation wavelengths of 441.6 and 488.0 nm. In other words, the contribution of carotenoid species showing higher v_1 frequencies, those around 1,531 cm^{-1} , increased with excitation wavelengths in this region. Table 2 lists the excitation energy dependences of the v_1 Raman frequencies with those bandwidths at the half maxima. Extremely large bandwidths of approximately 18–19 cm^{-1} were

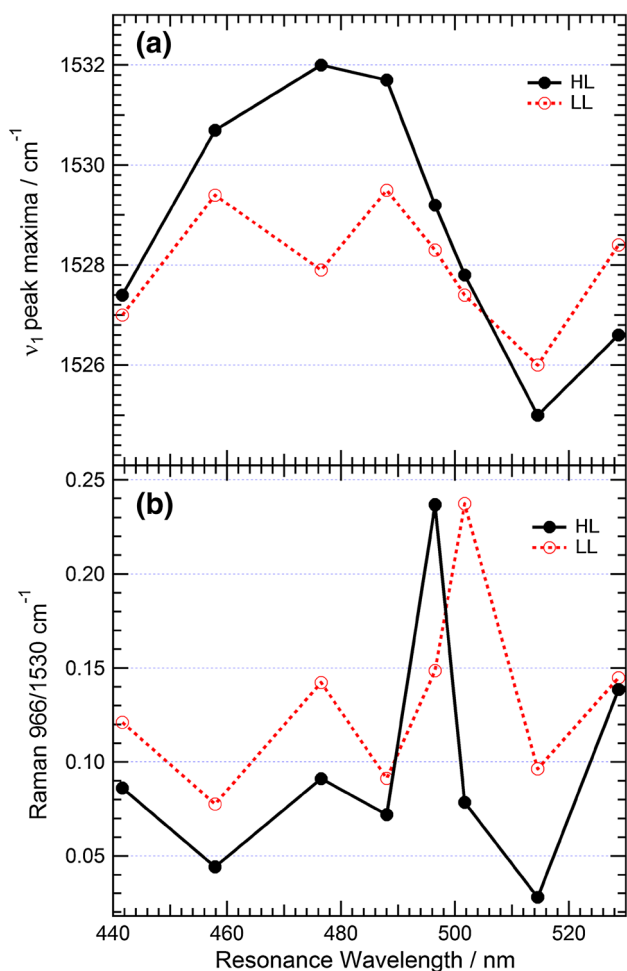


Fig. 6 **a** v_1 Raman frequencies and **b** amplitude of v_4 Raman lines relative to the v_1 Raman lines as a function of the excitation wavelengths for HL (closed circles and solid black line) and LL (open circles and red dashed line) intact filamentous *C. intricatum* cells

Table 2 v_1 Raman frequencies for intact filamentous *C. intricatum* cells cultivated under HL or LL

λ_{exc}/nm	v_1 frequency (fwhm ^a)/ cm^{-1}	
	HL	LL
441.6	1,527.4 (17.9)	1,527.0 (18.2)
457.9	1,530.7 (14.4)	1,529.4 (14.2)
476.5	1,532.0 (18.6)	1,527.9 (19.2)
488.0	1,531.7 (16.8)	1,529.5 (13.6)
496.5	1,529.2 (15.1)	1,528.4 (13.6)
501.7	1,527.8 (15.2)	1,527.4 (15.0)
514.5	1,525.0 (14.6)	1,526.0 (15.0)
528.7	1,525.0 (14.6)	1,528.4 (15.0)

^a Band width at half maxima of each v_1 Raman line was shown in cm^{-1} in parenthesis

observed when excited at 441.6 and 476.5 nm. The large bandwidth resulting from excitation at 441.6 nm can be explained by the effect of a nearby Raman band of Chl *a* at $1,560 \text{ cm}^{-1}$; the other large bandwidth resulting from excitation at 476.5 nm may indicate the contribution of many different carotenoids having slightly different v_1 frequencies. Based on the HPLC results, both tNx and tVx were more abundant in HL cells than in LL cells. The linear dependencies of the v_1 Raman lines on absorptive transitions have been reported (Mendes-Pinto et al. 2013); therefore, that both tNx and tVx resulted in the same absorption spectra (as shown in the Fig. 2b) could be attributed to the same v_1 Raman lines. The v_1 Raman line of tVx is reported to be around $1,528 \text{ cm}^{-1}$ in LHCII (Ruban et al. 2000) and around $1,530 \text{ cm}^{-1}$ in thylakoid membranes (Ruban et al. 2001). Consequently, the component that exhibited a v_1 frequency as high as $1,532 \text{ cm}^{-1}$ could have resulted from tNx, tVx, or both having weaker interactions with the proteins, which were more abundant when cells were grown in HL conditions.

The v_2 region of the Raman spectra is shown in Fig. 5c; this region is sensitive to the conformation of molecules (Koyama and Fujii 1999; Robert 2009). The Raman line at $1,136 \text{ cm}^{-1}$ (indicated by gray line in Fig. 5c) is highly characteristic of *9'-cis* isomer; this fingerprint was evident in both HL and LL spectra at each excitation wavelength ($1,132 \text{ cm}^{-1}$ in the reference of Snyder et al. (2004) for the *9'-cis* structure of Nx (9cNx in our abbreviation) in the LHCII binding site). A small but unambiguous enhancement of the amplitudes of $1,136 \text{ cm}^{-1}$ bands in LL spectra was observed when samples were excited with longer wavelengths, such as 501.7 and 514.5 nm. In order to quantify the *cis* contribution to the Raman signals, the relative intensity of the C10–C11 str. mode (at $1,136 \text{ cm}^{-1}$) to the C14–C15 str. mode (at $1,159 \text{ cm}^{-1}$) was calculated to be 0.06 (0.06) and 0.02 (0.05) for HL (LL) samples excited at 501.7 and 514.5 nm, respectively. The relative intensity ($1,136 \text{ cm}^{-1}/1,159 \text{ cm}^{-1}$) can be used as an indicator of the *cis* conformation of carotenoids, which is to be ~ 0.2 for the *9'-cis* isomer (Koyama and Fujii 1999). In LL cells, the relative intensity was between 0.05 and 0.06 and was slightly smaller than the reported values ~ 0.2 . These discrepancies may be due to the coexistence of all-*trans* forms of carotenoids, such as Vx, Sx, Sn, and α -carotene. This interpretation is in reasonable agreement with the HPLC results that showed the amount of 9cNx relative to total all-*trans* carotenoids was smaller in HL cells than in LL cells.

The v_3 regions of the Raman spectra are shown in Fig. 5b. Each band comprised four bands at 1,003, 1,006, 1,008, and 1,010 cm^{-1} . Several frequencies in this region have been empirically assigned to the xanthophylls bound to the LHCII; for example, 1,005–1,006 cm^{-1} indicates

Table 3 Assignment of absorptive transitions that occurred in intact filamentous *C. intricatum* cells

Assignment	442.0 ^a	453.5 ^b	465.0 ^a	476.5 ^a	486.5 ^b	487.5 ^a	500.0 ^a	542.0 ^a
Chls	Chl <i>a</i>			Chl <i>b</i>				
binding Sx/Sn				0–2 ^c			0–1 ^c	0–0 ^c
tVx/tNx		0–1 ^c			0–0 ^c			
9cNx			0–1 ^c			0–0 ^c		
			457.9 ^d			488.0 ^d		

^{a,b} Absorptive transitions (in nm) observed in the ^a second derivative spectra and ^b difference spectrum at 77 K (see Figs. 3b, c, respectively)

^c Empirically assigned vibrational transitions of the absorption spectrum (see text)

^d Excitation wavelength for the resonance Raman excitation profile (see Fig. 6a)

9cNx, 1,007 cm⁻¹ indicates Vx, 1,003–1,004 cm⁻¹ indicates lutein, and 1,003 cm⁻¹ indicates zeaxanthin (Ruban et al. 2001). We could safely assign the 1,006 cm⁻¹ band to 9cNx and 1,008 cm⁻¹ to Vx. *C. intricatum*, however, do not contain either lutein or zeaxanthin, but they do contain Sn/Sx and α -carotene. It is rather difficult to predict the frequencies of the methyl-rocking modes of unknown carotenoids only based on the structure; hence we could not assign the origin of either the 1,003 or 1,010 cm⁻¹ band.

The ν_4 regions of the Raman spectra are shown in Fig. 5a. Based on precise analysis, the ν_4 Raman patterns have been assigned to lutein bound to the aggregation/quenched state of the higher-plant type LHCII (Ruban et al. 2001). The ν_4 Raman patterns of HL samples were similar to the characteristic ν_4 Raman patterns of oligomeric LHCII (Fig. 5 in the reference of Ruban et al. 2000); these patterns include peaks at 953 and 965 cm⁻¹. The ν_4 Raman patterns of LL samples were similar to that of trimeric LHCII; in which the peak at 953 cm⁻¹ was eliminated. The excitation energy dependences of the amplitude of ν_4 band at 965 cm⁻¹ relative to those of the ν_1 band at 1,530 cm⁻¹ were plotted (Fig. 6b). The increases in relative intensities of the excitation at 476.5, 501.7, and 528.7 nm clearly corresponded to the peaks in the second-derivative spectra at 476.5, 500.0, and 542.0 nm, respectively. The differences between these absorptive transitions were $\sim 1,000$ cm⁻¹ for 476.5/500.0 nm peaks and $\sim 1,500$ cm⁻¹ for 500.0/542.0 nm peaks, indicating that those peaks represented a vibrational structure of the binding Sx/Sn. Table 3 summarizes the assignments of the absorptive transitions. Notably, all the ν_1 frequencies were around 1,528 cm⁻¹ when excited at these three excitation wavelengths (476.5/501.7/528.7 nm) (Fig. 6a); these observations confirmed that the ν_1 frequencies were indicative of Sx/Sn based on the similarity to the ν_1 frequencies of approximately 1,529 cm⁻¹ associated with fucoxanthin bound to FCP (vide infra, Premvardhan et al. 2009). The ν_4 patterns of these samples were very similar to those of lutein bound to LHC II (Ruban et al. 2000); consequently, we conclude that Sx/Sn occupies the similar

binding site in SCP that is normally occupied by lutein in LHCII. Sx has been considered to be biosynthesized from lutein by two-step oxidations. Actually the skeleton structure of Sx has many similarities with lutein. Therefore, the ν_4 modes may originate from the common modes shared by Sx, Sn, and lutein.

Plausible model of pigment regulation in response to HL irradiation

Under HL conditions, filamentous *C. intricatum* cells accumulate extra tNx and increased tVx and α -carotene. Additionally, low-temperature absorption spectra and the ν_4 modes of Raman lines indicated that antenna size increased under HL conditions. Nx is biosynthesized from Vx; therefore, Nx can be accumulated when Vx is accumulated. Vx can be overexpressed in order to enhance the xanthophyll cycle to protect against high light stress. However, tNx, tVx, or both that had accumulated in HL cells exhibited higher ν_1 frequencies; these findings indicate that interactions between these pigments and the proteins are weak. Therefore, the extra tNx and tVx may exist in the surface of the SCP to promote oligomerization of the SCP to control the amount of energy transferred from SCP to PSII by adjusting the distance between the energy donor and the energy acceptor in order to quench the excess amount of excitation energy.

Conclusion

We used a combination of second-derivative of low-temperature absorption spectroscopy and excitation wavelength dependence of resonance-Raman spectroscopy to investigate the absorptive transitions that occur in an intact filamentous cell of a siphonous green algae, *C. intricatum* OKAMURA. The absorption spectrum of the intact filamentous cells represents that of the major light-harvesting protein, SCP. Based on these analyses and especially on that of the ν_4 Raman patterns, we concluded that the

characteristic carbonyl carotenoids, Sx or Sn, may occupy the similar binding site in SCP that lutein normally occupies in LHCII.

Additionally, these cultured cells accumulate tNx as found in higher plant photosynthetic systems. This accumulation occurred only when cultures were exposed to extremely strong illumination (500 μ E). The tNx accumulation that occurred in HL cells was confirmed both by LC analysis of extracted pigments and by resonance Raman spectroscopy analysis of intact cells. The accumulation of tNx in HL cells was accompanied by the accumulation of Vx and α -carotene. Resonance Raman spectroscopy also indicated that the assembly of the SCP differed between LL and HL cells; specifically, the SCP was trimeric in LL cells and oligomeric in HL cells. We proposed a plausible model for adaptation to high-light conditions; nevertheless, the distribution of tNx and excess Vx in the SCPs must be investigated to test the validity of this hypothesis.

Acknowledgments This work was supported by Japan Society for the Promotion of Science (JSPS) KAKENHI Grant-in-Aid for JSPS fellows Numbers 254,691 to CU. This work was also supported by a Japan Science and Technology Agency (JST), Precursory Research for Embryonic Science and Technology (PRESTO) grant to RF. This work was partially supported by a Scientific Research on Innovative Areas “All Nippon Artificial Photosynthesis Project for Living Earth (AnApple)” Grant (No. 24107002) from the JSPS to HH. HH also thanks the Human Frontier Science Program for financial support.

References

- Anderson JM (1983) Chlorophyll-protein complexes of a *Codium* species, including a light-harvesting siphonaxanthin-chlorophyll *a/b*-protein complex, an evolution relic of some chlorophyta. *Biochim Biophys Acta* 724:370–380
- Andreeva A, Stoitchkova K, Busheva M, Apostolova E, Várkonyi Z, Garab G (2004) Resonance Raman spectroscopy of xanthophylls in pigment mutant thylakoid membranes of pea. *Biopolymers* 74:87–91
- Aruga Y, Inoue I, Tanaka J, Yokohama Y, Yoshida T (2000) In: Aruga Y, Inoue I, Tanaka J, Yokohama Y, Yoshida T (eds) *Sorui-gaku Enshu Jisshu*. Kodansha, Tokyo, pp 166–167
- Chu ZX, Anderson JM (1985) Isolation and characterization of a siphonaxanthin-chlorophyll *a/b* protein complex of photosystem I from a *Codium* species (Siphonales). *Biochim Biophys Acta* 806:154–160
- Jeffrey SW, Mantoura RFC, Bjørnland T (1997, 2005) Data for the identification of 47 key phytoplankton pigments. In: Jeffrey SW, Mantoura RFC, Wright SW (eds), *Phytoplankton pigments in oceanography guidelines to modern methods*, UNESCO, Spain, pp 449–559
- Koyama Y, Fujii R (1999) In: Frank HA, Young J, Britton G, Cogdell RJ (eds) *The photochemistry of carotenoids*. Kluwer Academic Publishers, Dordrecht, pp 161–187
- Mendes-Pinto MM, Sansiaume E, Hashimoto H, Pascal AA, Gall A, Robert B (2013) Electronic absorption and ground state structure of carotenoid molecules. *J Phys Chem B* 117:11015–11021
- Oka N, Kusumoto T, Taira T, Iha M, Shigematsu Y, Fujii R, Hashimoto H (2012) Novel mass production of siphonaxanthin from a green alga, “Motsure-miru” (*Codium intricatum*). *Carotenoid Sci* 17:19–22
- Premvardhan L, Bordes L, Beer A, Büchel C, Robert B (2009) Carotenoid structures and environments in trimeric and oligomeric fucoxanthin chlorophyll *a/c*₂ proteins from resonance Raman spectroscopy. *J Phys Chem B* 113:12565–12574
- Robert B (2009) Resonance Raman spectroscopy. *Photosynth Res* 101:147–155
- Ruban AV, Pascal AA, Robert B (2000) Xanthophylls of the major photosynthetic light-harvesting complex of plants: identification, conformation and dynamics. *FEBS Lett* 477:181–185
- Ruban AV, Pascal AA, Robert B, Horton P (2001) Configuration and dynamics of xanthophylls in light-harvesting higher plants. *J Biol Chem* 276:24862–24870
- Ruban AV, Berera R, Iliaia C, van Stokkum IHM, Kennis JTM, Pascal AA, van Amerongen H, Robert B, Horton P, van Grondelle R (2007) Identification of a mechanism of photoprotective energy dissipation in higher plants. *Nature* 450:575–579
- Snyder AM, Clark BM, Robert B, Ruban AV, Bungard RA (2004) Carotenoid specificity of light-harvesting complex II binding sites. *J Biol Chem* 279:5162–5168
- Takaichi S, Mimuro M (1998) Distribution and geometric isomerism of neoxanthin in oxygenic phototrophs: 9'-*cis*, a sole molecular form. *Plant Cell Physiol* 39:968–977
- Wang W, Qin X, Sang M, Chen D, Wang K, Lin R, Lu C, Shen JR, Kuang T (2013) Spectral and functional studies on siphonaxanthin-type light-harvesting complex of photosystem II from *Bryopsis corticulans*. *Photosynth Res* 117:267–279
- Yokohama Y (1983) A xanthophyll characteristic of deep-water green algae lacking siphonaxanthin. *Botanica Marina* 26(2):45–48